An ADMM Algorithm for Hybrid Variational Deblurring Model

Xiaojuan Yang†[1]

†.Jiangsu Key Laboratory for NSLSCS, School of Mathematical Sciences, Nanjing Normal University, Nanjing 210023, P. R. China
†.School of Mathematical Sciences, Nanjing Normal University, Taizhou College Taizhou, 225300, P. R. China

Abstract

In this paper, we propose a new method to solve a hybrid variational deblurring model for restoring blurred and noisy images. The hybrid model combines advantages of the first-order and second-order total variation. It can substantially reduce the staircase effect produced by the first-order total variation, while preserving sharp edges in the restored images. By introducing some auxiliary variables and splitting the variables two times, we obtain two equivalent constrained optimization formulations which are then addressed with the alternating direction method of multipliers (ADMM). Numerical results are given to illustrate the effectiveness of the proposed method.

Keywords: Image deblurring, total variation, alternating direction minimization of multipliers, split Bregman

1 Introduction

Image restoration such as denoising and deblurring is the most fundamental task in image processing. In this class of problems, a basic image restoration model is

$$f = Au + e,$$

where $u \in \mathbb{R}^{n^2}$ is the ideal $n \times n$ image, $f \in \mathbb{R}^{n^2}$ is the observed $n \times n$ image, $e \in \mathbb{R}^{n^2}$ is the zero-mean white Gaussian noise with variance σ^2 and $A \in \mathbb{R}^{n^2 \times n^2}$ represents a blurring (or convolution) operator.

One of the most basic and successful image regularization models is the ROF model first proposed by Rudin-Osher-Fatemi in [1], which reads

$$u = \arg\min_u \{R_{rof}(u) + \frac{\mu}{2}\|Au - f\|_2^2\}, \tag{1}$$

where

$$R_{rof}(u) = \|u\|_{TV} = \|\nabla u\|_1 = \sqrt{(\nabla_x u)^2 + (\nabla_y u)^2}$$

[1]Corresponding Author, email: yxjwyz@163.com

is the total variation (TV) regularization term, ∇ stands for the discrete gradient operator, $\|Au-f\|_2^2$ is the data fidelity term and $\mu > 0$ is the regularization parameter which provides a tradeoff between these two terms.

Many efficient methods have been proposed to solve (1). In [2], Chan, Golub, Mulet used Newton's linearization technique to solve a smoothed version of the primal-dual system for the ROF model. Based on the dual formulation, Chambolle [3] proposed a quite fast total variation minimization algorithm. Using Bregman iteration, Goldstein and Osher [4] gave a 'split Bregman' method, which can solve a very broad class of L1-regularized problems, including TV regularization minimization. By alternating minimization, Huang Y, NG, Wen Y [6] solved the following approximation to the model (1):

$$u = \arg\min_{w,u}\{\alpha\|\nabla w\|_1 + \frac{1}{2}\|w-u\|_2^2 + \frac{\mu}{2}\|Au-f\|_2^2\}.$$

Appling a quadratic penalty term, (1) is approximated in [5] by

$$u = \arg\min_{v,u}\{\|v\|_1 + \frac{\beta}{2}\|v-\nabla u\|_2^2 + \frac{\mu}{2}\|Au-f\|_2^2\},$$

and a corresponding alternating direction minimization (ADM) algorithm for this model was proposed and analyzed. Yang J, Zhang Y, Yin W [7] extended the ADM algorithm to the case of recovering blurry multichannel (color) images corrupted by impulsive rather than Gaussian noise.

Although the first-order TV-based ROF model (1) preserves edges well, the images resulting from this technique in the presence of noise are often piecewise constant, the so-called staircase effect; see [8–10, 12] and references therein. To overcome this staircase effect, high-order models have been considered [10, 13–16]. The Lysaker-Lundervold-Tai (LLT) model [15] first proposed by Lysaker, Lundervold and Tai, which reads

$$u = \arg\min_{u}\{R_{llt}(u) + \frac{\mu}{2}\|Au-f\|_2^2\}, \tag{2}$$

where

$$R_{llt}(u) = \|u\|_{HTV} = \|\nabla^2 u\|_1 = \sqrt{(\nabla_{xx}u)^2 + (\nabla_{xy}u)^2 + (\nabla_{yx}u)^2 + (\nabla_{yy}u)^2}$$

is the high total variation (HTV) regularization term.

The computational challenge of (2) mainly comes from the non-differentiability of the second-order regularization term $\|\nabla^2 u\|_1$. There have been several methods studied for the problem (2). Inspired by the work of Chambolle [3], Chen etal. [17] proposed a dual algorithm to solve the LLT model and experimental results indicated that the dual algorithm was faster than the original gradient desent algorithm. Hessian-based norm regularization methods were effectively used in [18] for image restoration problems and applied to biomedical imaging.

LLT model is known to recover smoother surfaces. Nevertheless, this model leads to poor edge-preserving performance. Hence, it is natural to utilize a combined first-order and second-order total variation technique to improve the image restoration capability.

In this paper, we consider to modify the total variation model by adding a high-order functional for restoring the blurring and noisy image. It leads to the following minimization problem:

$$\min_{u} \lambda\|\nabla u\|_1 + (1-\lambda)\|\nabla^2 u\|_1 + \frac{\mu}{2}\|Au - f\|_2^2, \tag{3}$$

where the weighted parameter $\lambda \in [0,1]$ is used to maintain a balance between artifact reduction and detail preservation. It is desirable that λ is 1 along edges and in flat regions, and should be almost close to 0 in homogeneous regions to suppress staircase effect.

The authors in [11] proposed a model for MR image reconstruction based on second order total variation regularization and wavelet, and they gave an algorithm which reduced a high-order problem to some lower-order problems with less computation. Inspired by the idea we use the variable splitting technique two times to reduce the hybrid model (3), and then apply the augmented Lagrangian method and split Bregman method to solve the reduced model.

This paper is organized as follows. In Section 2, we give our algorithm for (3) and it's convergence analysis. Numerical examples are presented in Section 3 to show the feasibility of the proposed model and algorithm.

2 The alternating direction method for the model (3)

We first introduce auxiliary variables $\omega = (\omega_1, \omega_2)^T$ subject to $\omega = \nabla u$ to transform $\nabla u = (\nabla_x u, \nabla_y u)^T$ out of the non-differentiable norms:

$$\min_{u,\omega} \lambda\|\omega\|_1 + (1-\lambda)\|\nabla\omega\|_1 + \frac{\mu}{2}\|Au - f\|_2^2, \quad s.t. \quad \omega = \nabla u, \tag{4}$$

where

$$\nabla\omega = \begin{pmatrix} \nabla_x\omega_1 & \nabla_y\omega_1 \\ \nabla_x\omega_2 & \nabla_y\omega_2 \end{pmatrix},$$

$$\|\nabla\omega\|_1 = \sqrt{(\nabla_x\omega_1)^2 + (\nabla_y\omega_1)^2 + (\nabla_x\omega_2)^2 + (\nabla_y\omega_2)^2}.$$

We form the augmented Lagrangian function:

$$
\begin{aligned}
L(u,\omega;b) = \lambda\|\omega\|_1 + (1-\lambda)\|\nabla\omega\|_1 + \frac{\rho_1}{2}\|\omega_1 - \nabla_x u - b_1\|_2^2 \\
+ \frac{\rho_1}{2}\|\omega_2 - \nabla_y u - b_2\|_2^2 + \frac{\mu}{2}\|Au - f\|_2^2
\end{aligned}
$$

to deal with the constrains in (4), where $b = (b_1, b_2) \in \mathbb{R}^{2n^2}$ is the Lagrangian multiplier, and ρ_1 is a positive penalty parameter. Started at $u = u^k$ and $b = b^k$, applying ADMM yields the iterative scheme

$$
\begin{cases}
(u^{k+1}, \omega^{k+1}) \leftarrow \arg\min\limits_{u,\omega} L(u,\omega;b^k), \\
b_1^{k+1} \leftarrow b_1^k + \gamma(\nabla_x u^{k+1} - \omega_1^{k+1}), \\
b_2^{k+1} \leftarrow b_2^k + \gamma(\nabla_y u^{k+1} - \omega_2^{k+1}).
\end{cases} \tag{5}
$$

Since the updates of b_1^k and b_2^k are merely simple calculations, we now focus on the minimization of $L(u,\omega;b^k)$ in (5), which can be divided into the following several subproblems:

$$
u^{k+1} = \arg\min_u \frac{\rho_1}{2}\|\omega_1^k - \nabla_x u - b_1\|_2^2 + \frac{\rho_1}{2}\|\omega_2^k - \nabla_y u - b_2\|_2^2 + \frac{\mu}{2}\|Au - f\|_2^2, \tag{6}
$$

$$
\begin{aligned}
(\omega_1^{k+1}, \omega_2^{k+1}) = \arg\min_{\omega_1,\omega_2} \lambda\|\omega\|_1 + (1-\lambda)\|\nabla\omega\|_1 + \frac{\rho_1}{2}\|\omega_1 - \nabla_x u^{k+1} - b_1^k\|_2^2 \\
+ \frac{\rho_1}{2}\|\omega_2 - \nabla_y u^{k+1} - b_2^k\|_2^2.
\end{aligned} \tag{7}
$$

We now investigate subproblem (6) and (7) in the following subsections.

2.1 u-subproblem

The minimization of L with respect to u is a least squares problem and the corresponding normal equation is:

$$
(\mu A^T A + \rho_1 \nabla_x^T \nabla_x + \rho_1 \nabla_y^T \nabla_y)u = \mu A^T f + \rho_1 \nabla_x^T(\omega_1^k - b_1^k) + \rho_1 \nabla_y^T(\omega_2^k - b_2^k).
$$

Since $\nabla_x^T \nabla_x + \nabla_y^T \nabla_y = -\Delta$, we get

$$
(\mu A^T A - \rho_1 \Delta)u = \mu A^T f + \rho_1 \nabla_x^T(\omega_1^k - b_1^k) + \rho_1 \nabla_y^T(\omega_2^k - b_2^k). \tag{8}
$$

We follow the standard assumption of $N(A) \cap N(\nabla) = 0$, where $N(\cdot)$ represents the null space of a matrix, which ensures the nonsingularity of the coefficient matrix in (8). It is known that under periodic boundary condition for u, both the Laplace operator and $A^T A$ are block circulant matrices with circulant blocks, see e.g., [19]. We can diagonalize the Hessian on the left hand side of (8) by the 2D discrete Fourier transforms $\mathcal{F}$. In order to facilitate the computation, we therefore compute u by one FFT (fast Fourier transform) and one IFFT (inverse fast Fourier transform). The specific iterative step is

$$u^{k+1} = \mathcal{F}^{-1}\left(\frac{\frac{\mu}{\rho_1}\mathcal{F}(A)^* \circ \mathcal{F}(f) + \mathcal{F}(\nabla)^* \circ \mathcal{F}(\omega^k - b^k)}{\frac{\mu}{\rho_1}\mathcal{F}(A)^* \circ \mathcal{F}(A) + \mathcal{F}(\nabla)^* \circ \mathcal{F}(\nabla)}\right), \tag{9}$$

where $*$ and $\circ$ denote complex conjugacy and elementwise multiplication respectively.

2.2 ω-subproblem

In order to solve the subproblem (7), we apply the split Bregman method [4] to ω-subproblem. We introduce three auxiliary variables p, v_1 and v_2 subject to $p = \nabla\omega, v_1 = \omega_1$ and $v_2 = \omega_2$. Then by using the operator splitting method [20, 21] to (7), we have the following iteration scheme

$$\begin{cases} (\omega_1^{k+1}, \omega_2^{k+1}, p^{k+1}, v_1^{k+1}, v_2^{k+1}) \leftarrow \arg \min\limits_{\omega_1,\omega_2,p,v_1,v_2} \lambda\|(v_1, v_2)\|_2 \\ +(1-\lambda)\|p\|_2 + \frac{\rho_2}{2}\|v_1 - \omega_1 - c_1^k\|_2^2 + \frac{\rho_2}{2}\|v_2 - \omega_2 - c_2^k\|_2^2 \\ +\frac{\rho_3}{2}\|p - \nabla\omega - d^k\|_2^2 + \frac{\rho_1}{2}\|\omega - \nabla u^{k+1} - b^k\|_2^2 \\ d_{11}^{k+1} = d_{11}^k + \gamma(\nabla_x\omega_1^{k+1} - p_{11}^{k+1}), \\ d_{12}^{k+1} = d_{11}^k + \gamma(\nabla_y\omega_1^{k+1} - p_{12}^{k+1}), \\ d_{21}^{k+1} = d_{21}^k + \gamma(\nabla_x\omega_2^{k+1} - p_{21}^{k+1}), \\ d_{22}^{k+1} = d_{22}^k + \gamma(\nabla_y\omega_2^{k+1} - p_{22}^{k+1}), \\ c_1^{k+1} = c_1^k + \gamma(\omega_1^{k+1} - v_1^{k+1}), \\ c_2^{k+1} = c_2^k + \gamma(\omega_2^{k+1} - v_2^{k+1}), \end{cases} \tag{10}$$

where d are the Lagrangian multipliers and c_1, c_2 are chosen through Bregman iteration:

$$d = \begin{pmatrix} d_{11} & d_{12} \\ d_{21} & d_{22} \end{pmatrix}, c = \begin{pmatrix} c_1 \\ c_2 \end{pmatrix},$$

and

$$v = \begin{pmatrix} v_1 \\ v_2 \end{pmatrix}, \|(v_1, v_2)\|_2 = \sqrt{v_1^2 + v_2^2},$$

$$p = \begin{pmatrix} p_{11} & p_{12} \\ p_{21} & p_{22} \end{pmatrix}, \|p\|_2 = \sqrt{p_{11}^2 + p_{12}^2 + p_{21}^2 + p_{22}^2}.$$

Next, we give the details of solving ω_1, ω_2 subproblems respectively.

2.2.1 ω_1- subproblem

According to (10), the solution of ω_1-subproblem is obtained by the following subproblems:

$$\begin{cases} \omega_1^{k+1} = \arg\min\limits_{\omega_1} \dfrac{\rho_1}{2}\|\omega_1 - \nabla_x u^{k+1} - b_1^k\|_2^2 + \dfrac{\rho_2}{2}\|v_1^k - \omega_1 - c_1^k\|_2^2 \\ +\frac{\rho_3}{2}\|p_{11}^k - \nabla_x\omega_1 - d_{11}^k\|_2^2 + \frac{\rho_3}{2}\|p_{12}^k - \nabla_y\omega_1 - d_{12}^k\|_2^2 \\ p_{11}^{k+1} = \arg\min\limits_{p_{11}}(1-\lambda)\|p\|_2 + \dfrac{\rho_3}{2}\|p_{11} - \nabla_x\omega_1^{k+1} - d_{11}^k\|_2^2, \\ p_{12}^{k+1} = \arg\min\limits_{p_{12}}(1-\lambda)\|p\|_2 + \dfrac{\rho_3}{2}\|p_{12} - \nabla_y\omega_1^{k+1} - d_{12}^k\|_2^2, \\ d_{11}^{k+1} = d_{11}^k + \gamma(\nabla_x\omega_1^{k+1} - p_{11}^{k+1}), \\ d_{12}^{k+1} = d_{12}^k + \gamma(\nabla_y\omega_1^{k+1} - p_{12}^{k+1}), \end{cases} \tag{11}$$

To solve the first minimization problem in (11), we differentiate with respect to ω_1 and set the result equal to zero, so we get the update rule

$$[(\rho_1+\rho_2)I + \rho_3(\nabla_x^T\nabla_x + \nabla_y^T\nabla_y)]\omega_1^{k+1} = rsh_1^k,$$

where

$$rsh_1^k = \rho_1(\nabla_x u^{k+1} + b_1^k) + \rho_2(v_1 - c_1^k) + \rho_3\nabla_x^T(p_{11}^k - d_{11}^k) + \rho_3\nabla_y^T(p_{12}^k - d_{12}^k)$$

represents the right-hand side in the above equation. We now take advantage of the identity $\nabla^T\nabla = -\triangle$ to get

$$[(\rho_1+\rho_2)I - \rho_3\triangle]\omega_1^{k+1} = rsh_1^k,$$

Therefore, the system that must be inverted to solve for ω_1^{k+1} is circulant. The above equation can be rewritten as

$$K\omega_1^{k+1} = rsh_1^k, \tag{12}$$

where

$$K = (\rho_1+\rho_2)I - \rho_3\triangle \tag{13}$$

represents the coefficient of the left-hand side in (12). We can use FFT to solve the system (12). For the second and third subproblems, despite the fact that the variables p_{11}, p_{12} do not decouple, we can explicitly solve the minimization problem for

Using a generalized shrinkage formula [22], $(p_{11}^{k+1}, p_{12}^{k+1})$ are expressed by:

$$\begin{aligned} p_{11}^{k+1} &= \max\left(s_1^k - \frac{1-\lambda}{\rho_3}, 0\right)\frac{\nabla_x\omega_1^{k+1} + d_{11}^k}{s_1^k}, \\ p_{12}^{k+1} &= \max\left(s_1^k - \frac{1-\lambda}{\rho_3}, 0\right)\frac{\nabla_y\omega_1^{k+1} + d_{12}^k}{s_1^k}, \end{aligned} \tag{14}$$

where

$$s_1^k = \sqrt{|\nabla_x \omega_1^{k+1} + d_{11}^k|^2 + |\nabla_y \omega_1^{k+1} + d_{12}^k|^2}.$$

The above shrinkage is extremely fast and requires only a few operations for per element of $(p_{11}^{k+1}, p_{12}^{k+1})$.

2.2.2 ω_2- subproblem

The solution of ω_2-subproblem is similar to that of ω_1-subproblem and can be obtained by the following subproblem:

$$\begin{cases} \omega_2^{k+1} = \arg\min\limits_{\omega_2} \dfrac{\rho_1}{2}\|\omega_2 - \nabla_y u^{k+1} - b_2^k\|_2^2 + \dfrac{\rho_2}{2}\|v_2^k - \omega_2 - c_2^k\|_2^2 \\ +\frac{\rho_3}{2}\|p_{21}^k - \nabla_x \omega_2 - d_{21}^k\|_2^2 + \frac{\rho_3}{2}\|p_{22}^k - \nabla_y \omega_2 - d_{22}^k\|_2^2 \\ p_{21}^{k+1} = \arg\min\limits_{p_{21}} (1-\lambda)\|p\|_2 + \dfrac{\rho_3}{2}\|p_{21} - \nabla_x \omega_2^{k+1} - d_{21}^k\|_2^2, \\ p_{22}^{k+1} = \arg\min\limits_{p_{22}} (1-\lambda)\|p\|_2 + \dfrac{\rho_3}{2}\|p_{22} - \nabla_y \omega_2^{k+1} - d_{22}^k\|_2^2, \\ d_{21}^{k+1} = d_{21}^k + \gamma(\nabla_x \omega_2^{k+1} - p_{21}^{k+1}), \\ d_{22}^{k+1} = d_{22}^k + \gamma(\nabla_y \omega_2^{k+1} - p_{22}^{k+1}), \end{cases} \tag{15}$$

According to the optimality conditions of (15), ω_2^{k+1} can be obtained by solving the system

$$K\omega_2^{k+1} = rsh_2^k \tag{16}$$

where K is defined in (13) and

$$rsh_2^k = \rho_1(\nabla_y u^{k+1} + b_y^k) + \rho_2(v_2 - c_2^k) + \rho_3 \nabla_x^T(p_{21}^k - d_{21}^k) + \rho_3 \nabla_y^T(p_{22}^k - d_{22}^k).$$

$(p_{21}^{k+1}, p_{22}^{k+1})$ can be get by the generalized shrinkage formula:

$$\begin{aligned} p_{21}^{k+1} &= \max\left(s_2^k - \frac{1-\lambda}{\rho_3}, 0\right)\frac{\nabla_x \omega_2^{k+1} + d_{21}^k}{s_2^k}, \\ p_{22}^{k+1} &= \max\left(s_2^k - \frac{1-\lambda}{\rho_3}, 0\right)\frac{\nabla_y \omega_2^{k+1} + d_{22}^k}{s_2^k}, \end{aligned} \tag{17}$$

where

$$s_2^k = \sqrt{|\nabla_x \omega_2^{k+1} + d_{21}^k|^2 + |\nabla_y \omega_2^{k+1} + d_{22}^k|^2}.$$

2.2.3 v- subproblem

We obtain v-subproblem by solving the following minimization problem

$$\begin{aligned} (v_1^{k+1}, v_2^{k+1}) = \arg\min_{v_1, v_2} \lambda\|(v_1, v_2)\|_2 + \frac{\rho_2}{2}\|v_1 - \omega_1^{k+1} - c_1^k\|_2^2 \\ + \frac{\rho_2}{2}\|v_2 - \omega_2^{k+1} - c_2^k\|_2^2 \end{aligned}$$

We can directly obtain the (v_1^{k+1}, v_2^{k+1}) by using the generalized shrinkage formula:

$$\begin{aligned} v_1^{k+1} &= \max\left(s_3^k - \frac{\lambda}{\rho_2}, 0\right)\frac{\omega_1^{k+1} + c_1^k}{s_3^k}, \\ v_2^{k+1} &= \max\left(s_3^k - \frac{\lambda}{\rho_2}, 0\right)\frac{\omega_2^{k+1} + c_2^k}{s_3^k}, \end{aligned} \tag{18}$$

where

$$s_3^k = \sqrt{|\omega_1^{k+1} + c_1^k|^2 + |\omega_2^{k+1} + c_2^k|^2}.$$

Below we give our algorithm for solving the hybrid model (3).

Algorithm 1 The alternating direction method for the model (3)

1.Input $f, A, \mu > 0$, and $\rho_1, \rho_2, \rho_3 > 0$. Initialize $u^0 = f$ and $b_1^0 = b_2^0$ $= c_1^0 = c_2^0 = d_{ij}^0 = p_{ij}^0 = v_1^0 = v_2^0 = 0, i, j = 1, 2.$

2.While $\frac{\|u^k - u^{k+1}\|}{\|u^k\|} > tol$ Do

(1) Compute u^{k+1} according to (9);

(2) Compute ω_1^{k+1} according to (12);

Compute ω_2^{k+1} according to (16);

(3) Compute p_{ij}^{k+1} according to (14) and (17);

(4) Compute v_1^{k+1}, v_2^{k+1} according to (18);

(5) Update $b_1^{k+1}, b_2^{k+1}, c_1^{k+1}, c_2^{k+1}$ and d_{ij}^{k+1} according to (5) and (10).

End Do

Our method is equivalent to the minimization:

$$\begin{aligned} \min_u \lambda\|(v_1, v_2)\|_1 + (1-\lambda)\|p\|_1 + \frac{\mu}{2}\|Au - f\|_2^2, \\ s.t. v_1 = \omega_1, v_2 = \omega_2, p = \nabla\omega. \end{aligned} \tag{19}$$

Let

$$E = \begin{pmatrix} \nabla_x \\ \nabla_y \\ 0 \\ 0 \\ 0 \\ 0 \\ 0 \\ 0 \end{pmatrix}, F_1 = \begin{pmatrix} -I \\ 0 \\ 0 \\ -I \\ \nabla_x \\ \nabla_y \\ 0 \\ 0 \end{pmatrix}, F_2 = \begin{pmatrix} 0 \\ -I \\ 0 \\ -I \\ 0 \\ 0 \\ \nabla_x \\ \nabla_y \end{pmatrix}, G_1 = \begin{pmatrix} 0 \\ 0 \\ 0 \\ 0 \\ -I \\ 0 \\ 0 \\ 0 \end{pmatrix}, G_2 = \begin{pmatrix} 0 \\ 0 \\ 0 \\ 0 \\ 0 \\ -I \\ 0 \\ 0 \end{pmatrix},$$

$$G_3 = \begin{pmatrix} 0 \\ 0 \\ 0 \\ 0 \\ 0 \\ 0 \\ -I \\ 0 \end{pmatrix}, G_4 = \begin{pmatrix} 0 \\ 0 \\ 0 \\ 0 \\ 0 \\ 0 \\ 0 \\ -I \end{pmatrix}, H_1 = \begin{pmatrix} 0 \\ 0 \\ I \\ 0 \\ 0 \\ 0 \\ 0 \\ -I \end{pmatrix}, H_2 = \begin{pmatrix} 0 \\ 0 \\ 0 \\ I \\ 0 \\ 0 \\ 0 \\ -I \end{pmatrix},$$

Then we can rewritten the constrains of the minimization problem (19) as

$$Eu + F_1\omega_1 + F_2\omega_2 + G_1p_{11} + G_2p_{12} + G_3p_{21} + G_4p_{22} + H_1v_1 + H_2v_2 = 0.$$

Since our method is basically an application of ADMM for the case with four blocks of variables u, (ω_1, ω_2), $(p_{11}, p_{12}, p_{21}, p_{22})$ and (v_1, v_2), its convergence is guaranteed by the results of ADMM in [25].

3 Numerical experiments

In this section, we present some experiments to illustrate the performance of our proposed algorithm to solve image restoration problems. All the codes are written with MATLAB 7.7 (R2008b), and run on an Intel Pentium Dual CPU at 2.60 GHz and 2GB of memory.

We measure the quality of the restoration results with different methods by the peak signal-to-noise ratio (PSNR) and the relative error (ReErr) with

$$\mathrm{PSNR} = 20\log_{10}\frac{u_{max}}{\sqrt{Var(u,f^*)}},$$

where

$$\mathrm{Var}(u, f^*) = \frac{\sum_{j=0}^{n-1}[f^*(j)-u(j)]^2}{n},$$

and

$$\mathrm{ReErr} = \frac{\|u-f^*\|_2}{\|f^*\|_2},$$

where f^* is the orginal image, u is the restored image, $\tilde{f}$ is the mean intensity value of f^* and u_{max} is the maximum possible pixel value of the image u.

In order to better measure the similarity between two images, a well-known quality metric introduced by Wang et al. [23], the structure similarity (SSIM) indexe is defined as follows:

$$\mathrm{SSIM} = \frac{(2\mu_f^*\mu_u+C_1)(2\sigma_{f^*u}+C_2)}{(\mu_{f^*}^2+\mu_u^2+C_1)(\sigma_{f^*}^2+\sigma_u^2+C_2)},$$

where μ_{f^*} and μ_u are averages of f^* and u respectively, σ_{f^*} and σ_u are the variance of f^* and u respectively, σ_{f^*u} is the covariance of f^* and u and the positive constants C_1 and C_2 can be thought of as stabilizing constants for near-zero denominator values. The SSIM map is whiter, the restored image is closer to the clean image.

To make it easier to compare different methods, a uniform stopping criterion is used for all the algorithms we tested, that is,

$$\frac{\|u^{k+1} - u^k\|}{\|u^{k+1}\|} < 10^{-4},$$

where u^k is the restored image of the respective model in the kth iteration. In all tests, the periodic boundary condition is used to generate the convolution operator.

We all know that the quality of the restored image depends on the value of the regularization parameter μ. We tune it manually and choose the one that give higher PSNR value. Regarding the penalty parameters in all methods, it has been proven in [24] that theoretically any positive values of penalty parameters ensure the convergence of ADMM. We try some values and pick a value with satisfactory performance and then fix it.

In this experiment, we compare our method with the two methods proposed in [5] (FTVd) and in [6] (Fast TV). Here, the FTVd algorithm used for comparison is FTVd-v4.1, which is the latest version of FTVd. The experiments are made with clean images Barbara, Elaine, House and Hedgebw. Two blur kernels $G([7,7],4)$ and $M(40,10)$ are used on the clean images, which are further corrupted by Gaussian noise with zero mean and standard deviation of size 10^{-3} and 10^{-1} respectively. In the three methods, γ is set to 1.618, and the penalty parameters are $\rho_1 = 0.01, \rho_2 = 0.01, \rho_3 = 0.01$ in Algoritnm 1, $\beta = 0.01$ in FTVd, and $\alpha = 0.1$ in Fast TV respectively. The regularization parameter μ and the weighted parameter λ of different image restoration methods are presented in Table 1.

Table 1 The regularization parameters and the weighted parameters

Image	σ	two types of blur							
		Gaussian ([7,7],4)				Motion(40,10)			
		μ							
		FTVd	Fast TV	Our method(λ)		FTVd	Fast TV	Our method(λ)	
Barbara	10^{-3}	7×10^6	2×10^6	1×10^7	(0.5)	8×10^6	4×10^6	8×10^6	(0.3)
Elaine	10^{-3}	7×10^6	2×10^6	2×10^7	(0.4)	1×10^7	3×10^6	1×10^7	(0.7)
House	10^{-1}	1×10^3	1×10^2	1×10^3	(0.8)	1×10^3	5×10^1	9×10^2	(0.8)
Hedgebw	10^{-1}	2×10^3	7×10^1	3×10^3	(0.5)	2×10^3	7×10^1	3×10^3	(0.5)

In Table 2, we list the the PSNR, SSIM and ReErr values of restored images for FTVd, Fast TV and our method . We see that our method obtains the best PSNR, SSIM and ReErr values. The restored images of all methods are shown in Fig1-6. Fig1-3 and Fig 4-6 correspond to the images corrupted by Gaussian noise with zero mean and standard deviation of size 10^{-3} and 10^{-1} respectively. We display the zoomed parts of the restored Barbara and

Elaine images in Fig2 and 3. In Fig4, it is seen that the SSIM map of the restored image obtained by our method is slightly whiter than those by the other methods, i.e., our method can get better restoration results.

Table 2 Output of the experiments

Image	σ	Method	two types of blur					
			Gaussian ([7,7],4)			Motion(40,10)		
			PSNR	SSIM	ReErr	PSNR	SSIM	ReErr
		FTVd	50.23	0.9982	0.0052	53.90	0.9990	0.0034
Barbara	10^{-3}	Fast TV	48.45	0.9968	0.0064	50.16	0.9977	0.0053
		Our method	**51.45**	**0.9986**	**0.0045**	**54.82**	**0.9992**	**0.0031**
		FTVd	49.06	0.9970	0.0059	52.79	**0.9987**	0.0039
Elaine	10^{-3}	Fast TV	47.60	0.9957	0.0070	50.53	0.9978	0.0050
		Our method	**49.36**	**0.9972**	**0.0057**	**52.88**	**0.9987**	**0.0038**
		FTVd	37.68	0.9497	0.0389	37.71	0.9484	0.0287
House	10^{-1}	Fast TV	34.68	0.8846	0.0399	33.79	0.8808	0.0442
		Our method	**38.24**	**0.9526**	**0.0274**	**38.00**	**0.9504**	**0.0277**
		FTVd	32.91	0.9392	0.0591	33.28	0.9394	0.0562
Hedgebw	10^{-1}	Fast TV	31.87	0.9220	0.0642	31.23	0.9080	0.0691
		Our method	**33.81**	**0.9482**	**0.0535**	**34.06**	**0.9481**	**0.0510**

(a) Ideal image (b) Blurred and noisy image

(c) FTVd (d) Fast TV (e) Our method

Figure 1: Comparison of FTVd, Fast TV and our method on Barbara image in the case of Gaussian blur $G([7,7],4)$ and Gaussian noise with standard deviation of size 10^{-3}.

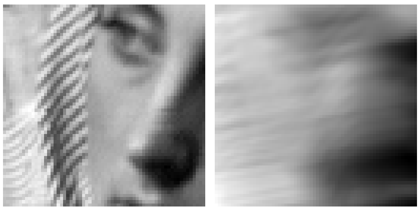

(a) Ideal image (b) Blurred and noisy image

(c) FTVd (d) Fast TV (e) Our method

Figure 2: Comparison of FTVd, Fast TV and our method on the partial enlargment of Barbara image in the case of motion blur $M(40, 10)$ and Gaussian noise with standard deviation of size 10^{-3}.

(a) Ideal image (b) Blurred and noisy image

(c) FTVd (d) Fast TV (e) Our method

Figure 3: Comparison of FTVd, Fast TV and our method on Elaine image in the case of Gaussian blur $G([7, 7], 4)$ and Gaussian noise with standard deviation of size 10^{-3}.

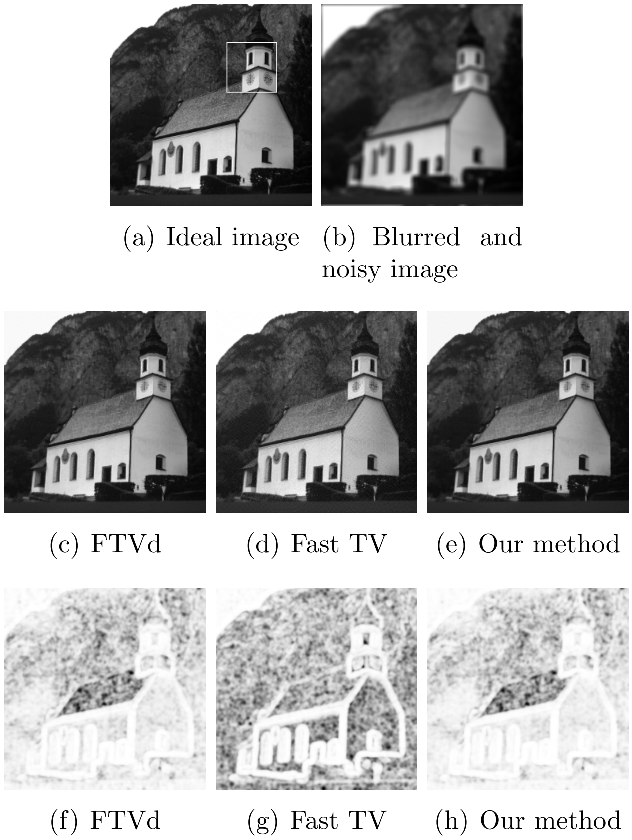

Figure 4: Comparison of FTVd, Fast TV and our method on House image in the case of Gaussian blur $G([7,7],4)$ and Gaussian noise with standard deviation of size 10^{-1}.

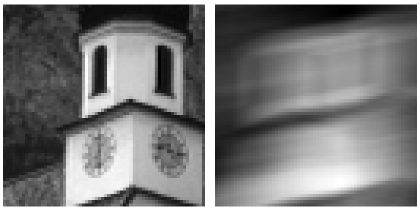

(a) Ideal image (b) Blurred and noisy image

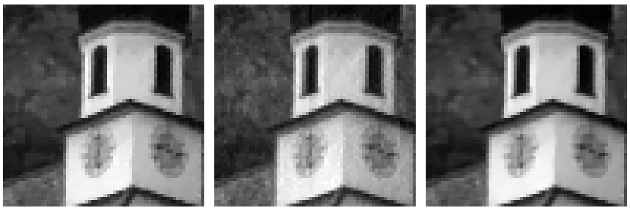

(c) FTVd (d) Fast TV (e) Our method

Figure 5: Comparison of FTVd, Fast TV and our method on the partial enlargment of House image in the case of motion blur $M(40, 10)$ and Gaussian noise with standard deviation of size 10^{-1}.

(a) Ideal image (b) Blurred and noisy image

(c) FTVd (d) Fast TV (e) Our method

Figure 6: Comparison of FTVd, Fast TV and our method on Hedgebw image in the case of Gaussian blur $G([7, 7], 4)$ and Gaussian noise with standard deviation of size 10^{-1}.

4 Conclusions

In this paper, we consider a hybrid variational deblurring model for restoring blurred images corrupted by Gaussian noise. We propose a new alternating direction method based on splitting the variables two times to obtain two equivalent constrained optimization formulations. The proposed method combines advantages of the first-order and second-order total variation. The numerical experiments show that the proposed method outperforms some existing restoration methods in terms of the PSNR, RelErr and SSIM map for Gaussian blur and noise removal problem.

References

[1] L. I. Rudin, S.Osher and E. Fatemi, "Nonlinear total variation based noise removal algorithms," Physica D: Nonlinear Phenomena, vol.60, no. 1, 1992, pp. 259-268.

[2] T. F. Chan, G. H. Golub and P. Mulet, "A nonlinear primal-dual method for total variation-based image restoration," SIAM Journal on Scientific Computing, vol. 20, no. 6, 1999, pp. 1964-1977.

[3] A. Chambolle, "An algorithm for total variation minimization and applications," Journal of Mathematical Imaging and Vision, vol. 20, 2004, pp. 89-97.

[4] T.Goldstein and S. Osher, "The split Bregman method for L1-regularized problems," SIAM Journal on Imaging Sciences, vol. 2, no. 2, 2009, pp. 323-343.

[5] Y. Wang, J. Yang and W. Yin, et al., "A new alternating minimization algorithm for total variation image reconstruction," SIAM Journal on Imaging Sciences, vol. 1, no. 3, 2008, pp. 248-272.

[6] Y. Huang, M. K. Ng and Y. W.Wen, "A fast total variation minimization method for image restoration," Multiscale Modeling and Simulation, vol. 7, no. 2, 2008, pp. 774-795.

[7] J. Yang, Y. Zhang and W. Yin, "An efficient TVL1 algorithm for deblurring multichannel images corrupted by impulsive noise," SIAM Journal on Scientific Computing, vol. 31, no. 4, 2009, pp. 2842-2865.

[8] A. Buades, B. Coll and J. M.Morel, "The staircasing effect in neighborhood filters and its solution," Image Processing, IEEE Transactions, vol. 15, no. 6, 2006, pp. 1499-1505.

[9] T. Chan, S. Esedoglu and F. Park, et al., "Recent developments in total variation image restoration," Mathematical Models of Computer Vision, 2005.

[10] T. Chan, A. Marquina and P. Mulet, "High-order total variation-based image restoration," SIAM Journal on Scientific Computing, vol. 22, no. 2, 2000, pp. 503-516.

[11] W. S, Xie, Y. F. Yang and B. Zhou, "An ADMM algorithm for second-order TV-based MR image reconstruction," Numerical Algorithms, 2014, pp. 1-17.

[12] J. Weickert, " Anisotropic diffusion in image processing," Stuttgart: Teubner, 1998.

[13] X. G, Lv, Y. Z. Song and S. X. Wang, et al., "Image restoration with a high-order total variation minimization method," Applied Mathematical Modelling, vol. 37, no. 16, 2013, pp. 8210-8224.

[14] M. Benning, C. Brune and M. Burger, et al., "Higher-order TV methods enhancement via Bregman iteration," Journal of Scientific Computing, vol. 54, no. 2-3, 2013, pp. 269-310.

[15] M. Lysaker, A. Lundervold and X. C. Tai, "Noise removal using fourth-order partial differential equation with applications to medical magnetic resonance images in space and time," Image Processing, IEEE Transactions, vol. 12, no. 12, 2003, pp. 1579-1590.

[16] T. F. Chan, S. Esedoglu and F. Park, "A fourth order dual method for staircase reduction in texture extraction and image restoration problems,"Image Processing (ICIP), 2010, pp. 4137-4140.

[17] H. Chen, J. Song and X. C. Tai, "A dual algorithm for minimization of the LLT model," Advances in Computational Mathematics, vol. 31, no. 1-3, 2009, pp. 115-130.

[18] S. Lefkimmiatis, A. Bourquard and M. Unser "Hessian-based norm regularization for image restoration with biomedical applications," Image Processing, IEEE Transactions, vol. 21, no. 3, 2012, pp. 983-995.

[19] M. K. Ng, R. H. Chan and W. C. Tang, "A fast algorithm for deblurring models with Neumann boundary conditions," SIAM Journal on Scientific Computing, vol. 21, no. 3, 1999, pp. 851-866.

[20] J. Eckstein and D. P.Bertsekas, "On the douglasrachford splitting method and the proximal point algorithm for maximal monotone operators," Mathematical Programming, vol. 55, no. 1-3, 1992, pp. 293-318.

[21] S. Setzer, "Split Bregman algorithm, Douglas-Rachford splitting and frame shrinkage," Scale space and variational methods in computer vision. Springer Berlin Heidelberg, 2009, pp. 464-476.

[22] Y. Wang, W. Yin and Y. Zhang, "A fast algorithm for image deblurring with total variation regularization," 2007.

[23] Z. Wang, A. C. Bovik and H. R. Sheikh, et al., "Image quality assessment: from error visibility to structural similarity," Image Processing, IEEE Transactions, vol. 13, no. 4, 2004, pp. 600-612.

[24] B. He, H. Yang, "Some convergence properties of a method of multipliers for linearly constrained monotone variational inequalities," Operations research letters, vol. 23, no. 3, 1998, pp. 151-161.

[25] M. Hong, Z. Q. Luo, "On the linear convergence of the alternating direction method of multipliers," arXiv preprint arXiv:1208.3922, 2012.